Int. J. Multiphase Flow Vol. 17, No. 5, pp. 599–619, 1991
Printed in Great Britain

0301-9322/91 $3.00 + 0.00
Pergamon Press/Elsevier

DIRECT CONTACT CONDENSATION AND MOMENTUM TRANSFER IN TURBULENT SEPARATED FLOWS

E. D. HUGHES and R. B. DUFFEY†
Idaho National Engineering Laboratory, EG&G Idaho Inc., Idaho Falls, ID 83415, U.S.A.

(Received 19 November 1990; in revised form 5 May 1991)

Abstract—Analysis of the turbulent velocity and shear stress distribution in a separated two-phase flow shows that both the wall and interface shear contribute to the dissipation of energy in the liquid film. A suitably averaged turbulent energy dissipation provides Kolmogorov velocity and length scales in the liquid film. These scales are used in a turbulent eddy based surface renewal theory for condensation and evaporation of saturated vapor onto or from its liquid. The theory accurately predicts experimental data for horizontal, concurrent condensation of steam on water. Theoretical results agree with the form of existing turbulent correlations for heat and mass transfer processes such as condensation onto a falling liquid film and mass, momentum and heat transfer at the interface in separated flows. Comparison of the theory to previous work is included and guidelines for empirical correlations of data are given.

Key Words: condensation, heat transfer, turbulence, dissipation

1. INTRODUCTION

1.1. Literature review

Heat, mass and momentum exchange at the interface between a gas (or vapor) and a liquid is encountered in industrial processes and natural phenomena. Heating and evaporation of a liquid film and condensation of a vapor onto its liquid occur in heat exchange equipment. Condensation and phase change is of interest in direct contact condensation (Cook *et al.* 1981; Berry & Goss 1972; Bankoff *et al.* 1981,1982; Lee *et al.* 1979; Lim *et al.* 1981,1984; Bankoff & Kim 1985; Chen *et al.* 1987). The rate of condensation depends on the turbulence level in the liquid, where turbulent eddies transport the heat away from the interface. The energy for turbulence production is obtained from shear at both the wall and interface. The same idea holds for gas absorption into liquid and for heating and evaporation of liquid films.

Gas absorption into a liquid is encountered in chemical processing applications. Gas absorption into oceans, lakes and rivers is important relative to determination of the effects of pollution on the environment. Interest in the momentum transfer problem lies in water and gas mass transport in oceans, reservoirs, channels and flumes, a subject of interest also to civil and geophysical engineering (Hidy & Plate 1966; Tsanis 1989; Koutitas & O'Connor 1980; Rastogi & Rodi 1978; Ueda *et al.* 1977; Fortescue & Pearson 1967). We discuss the coupling between mass and momentum transfer for relatively shallow flows in this paper, and examine deep oceans in a later paper (Duffey & Hughes 1991). The effect of interfacial shear on the mass transfer rate has been investigated by Chung & Mills (1974,1976) and Henstock & Hanratty (1979); and interfacial shear effects on falling film heat transfer by Hubbard *et al.* (1976).

The detailed characteristics of the turbulence near a vapor–liquid interface are of particular interest for the case of mass absorption into a liquid. Some experimental investigations have been conducted, but the exact nature of turbulence at the interface has not yet been determined. Jepsen *et al.* (1966) have determined the diffusivity distribution for falling films without interfacial shear. Their data show the diffusivity approaching the molecular value near the interface. Jeffries *et al.* (1970) investigated stratified flows with interfacial shear and concluded that the turbulence intensity does not fall to zero near the interface. Ueda *et al.* (1977) found the distributions of eddy diffusivity for momentum and heat to be parabolic and approach zero near the interface for open channel flow without interfacial shear.

†Present address: Brookhaven National Laboratory, Upton, NY 11973, U.S.A.

We provide a theory based on renewal concepts for the flow of a turbulent liquid with a turbulent gas, as in wind over water, falling film flows, horizontal separated flows, or annular flow in pipes. The exchange process is controlled by turbulence in the liquid, and we derive the time scale for eddy renewal based on the dissipation caused by wall and interfacial shear.

What has been shown in previous studies is that the eddy diffusivity for momentum can be treated as parabolic (e.g. Ueda *et al.* 1977; Mudawwar & El-Masri 1986; Shmerler & Mudawwar 1988a,b; Tsanis 1989); that the wall shear is close to that for classic pipe or plane flows (Ueda *et al.* 1977); and that many and various parabolic eddy diffusivity profiles may be fitted or adopted. Limberg (1973), for example, used the eddy diffusivity profiles directly from pipe flows. The intersection of diffusivity profiles from the wall and the interface has been used by Mills & Chung (1973), Hubbard *et al.* (1976) and Seban & Faghri (1976) as a means to establish a complete profile. The eddy diffusivity from gas absorption studies (Lamourelle & Sandall 1972; Chung & Mills 1974) has been used near the interface, and is assumed to represent the near interface conditions because of the importance of the interface to gas absorption. Levich (1962) postulated that surface tension at the interface provides for damping of the diffusivity there. This model has been used in studies of gas absorption by Lamourelle & Sandall (1972), Davies and coworkers (Davies & Ting 1967; Davies & Warner 1969; Davies & Hameed 1971) and Chung & Mills (1976), and in falling film heat transfer and evaporation by Mills & Chung (1973) and Seban & Faghri (1976), among others. We use this earlier work in developing a parabolic mixing length model in the film.

1.2. Physical phenomena and model assumptions

An idealized representation of a separated flow is given in figure 1, which shows a flow of a gas or vapor adjacent to a liquid. The flow may be horizontal or vertical, and we consider the case of cocurrent turbulent flow in both the liquid and gas. Figure 1 is highly idealized, in that vigorous interaction between the fluids occurs at the interface. Wave formation, breakup and liquid entrainment provide for increased area between the fluids, and can result in enhanced heat, mass and momentum exchange. The structure of the interface affects the interface shear, the presence of waves affects mass transfer (Jepsen *et al.* 1966; Banerjee *et al.* 1968; Davies & Warner 1969; Brumfield *et al.* 1975) and surface tension at the interface decreases turbulence production there (Levich 1962; Won & Mills 1982). We adopt an interface shear correlation to model these roughness effects at the macroscopic level.

The exchange process at the interface is controlled by molecular diffusion into the liquid, which is at the bulk state because it is transported to the interface by turbulent eddies. Surface renewal theory predicts the mass transfer coefficient, k_L, is (Higbie 1935):

$$k_L \sim \sqrt{D_m}\sqrt{\frac{1}{t_{rp}}}, \qquad [1a]$$

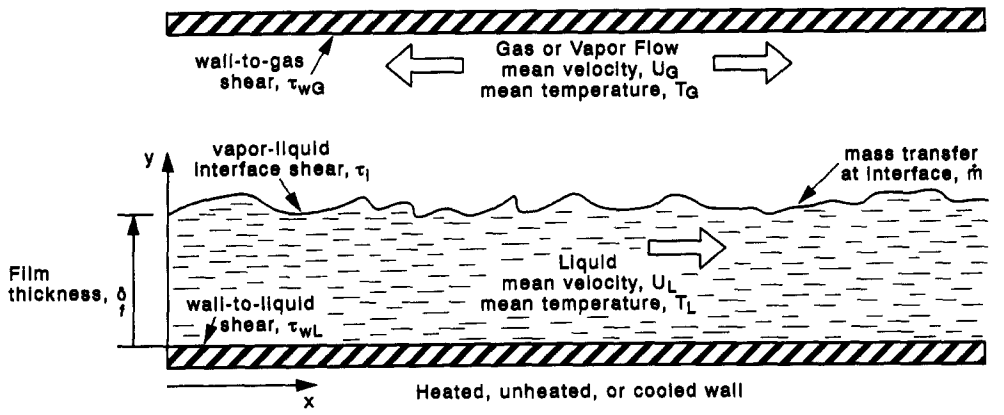

Figure 1. An idealized two-phase separated flow (horizontal or vertical).

where D_m is the molecular diffusivity of mass and t_{rp} is the renewal period, which is related to a characteristic velocity, V_c, and a length scale, L_c, by

$$t_{rp} = \frac{L_c}{V_c}. \qquad [1b]$$

The heat transfer coefficient also depends on these scales.

Various physical quantities have been used for the velocity and length scales. The length scale has been variously taken to be the film thickness (Henstock & Hanratty 1979), the wave amplitude (Banerjee *et al.* 1968), a characteristic macroscale of the flow (Fortescue & Pearson 1967) and a fraction of the diameter of the flow channel. The velocity scale has been taken as the wave velocity (Banerjee *et al.* 1968), the shear velocity (Henstock & Hanratty 1979; Davies 1972), turbulence intensity (Fortescue & Pearson 1967), the Kolmogorov length scale (Lamont & Scott 1970) and a fraction of the mean velocity. Banerjee *et al.* (1968) related the dissipation in the Kolmogorov scales to mean flow characteristics such as wave amplitude and velocity. Theofanous and coworkers (Theofanous *et al.* 1976; Brumfield *et al.* 1975; Brumfield & Theofanous 1976; Theofanous 1984) have developed an approach based on observed flow field and wave properties. We take length and velocity scales derived from analysis of the dissipation in turbulent film flows.

In the remainder of this paper, surface renewal theory is applied to obtain a description of the effects of wall and interfacial shear and the eddy diffusivity distribution on heat and mass transfer. The heat and mass transfer are directly derived from the momentum transfer.

The theoretical developments are given in section 2. In section 3, the theoretical results are applied to predictiosn of heat transfer and condensation data; the conclusions of the study are given in section 4.

2. THEORY DEVELOPMENT

The major elements in our modeling of separated and film flows are: (1) surface renewal theory for diffusion into the liquid at the interface; (2) the turbulence characteristics of the liquid; and (3) overall mass, momentum and energy balance equations for the bulk flow of the two-phase mixture. The coordinate system and additional notational information have been given in figure 1.

The theoretical development is based on the assumptions that: (1) the liquid and vapor are incompressible and the flow is steady in time; (2) surface curvature effects are small and negligible; (3) turbulence characteristics are obtainable from mixing length and turbulent eddy viscosity models, when the vapor–liquid interface may be smooth or roughened by surface waves; and (4) the wall-to-liquid and wall-to-vapor interfaces are treated by friction factors as in single-phase flow. These assumptions are reasonable and are justified by comparisons with experimental data.

2.1. Surface renewal theory

The surface renewal theory reduces the transfer problem to the determination of a single parameter; the rate of renewal of the gas–liquid interface by the flow characteristics of the liquid. The various estimates of the velocity and length scales that appear in the renewal period have been summarized above.

The present approach builds on the classic earlier work referenced above in several key respects. Firstly, the turbulence properties are coupled to the renewal period, t_{rp}, via characteristic length, L_c, and velocity, V_c, scales. Secondly, these scales are directly related to the dissipation, which is governed by the stress due to *both* the wall and interface shear.

In our modeling we take a shear stress distribution which is linear and fits the boundary conditions; the shear stress is coupled to the dissipation via homogeneous isotropic turbulence velocity and length scales; and the dissipation is taken as the average value, so the wall and interface contributions are obtained naturally.

From surface renewal theory the heat flux at the interface (Banerjee 1978) is

$$q_{iGL} = 2\rho_L c_{pL}\left(\frac{\alpha_{tL}}{\pi}\right)^{1/2}\left(\frac{1}{t_{rp}}\right)^{1/2}(T_{sat} - T_L), \qquad [2a]$$

where α_{tL} is the liquid thermal diffusivity and t_{rp} is the duration of the renewal period. The heat transfer coefficient is

$$h_c = \frac{q_{iGL}}{(T_{sat} - T_L)} = 2\rho_L c_{pL}\left(\frac{\alpha_{tL}}{\pi}\right)^{1/2}\left(\frac{1}{t_{rp}}\right)^{1/2}. \quad [2b]$$

The corresponding result for the mass transfer problem is [1a] above.

We determine the renewal period by use of the Kolmogorov length and velocity scales and dissipation of energy in the liquid. The length scale is $L_C = (\nu_L^3/\epsilon)^{1/4}$, the velocity scale is $V_C = (\nu_L \epsilon)^{1/4}$ and thus the renewal period is $t_{rp} = (\nu_L/\epsilon)^{1/2}$, where ϵ is the dissipation per unit mass of liquid, and [2b] becomes

$$h_c = 2\rho_L c_{pL}\left(\frac{\alpha_{tL}}{\pi}\right)^{1/2}\left(\frac{\epsilon}{\nu_L}\right)^{1/4}. \quad [3]$$

2.2. Turbulence characteristics of sheared liquid-film flows

The turbulence characteristics of the liquid can be described using the time-averaged boundary layer equations incorporating the Reynolds stress due to velocity fluctuations (Schlichting 1979; Landahl & Mollo-Christensen 1986). For the flow shown in figure 1, the mass conservation is

$$\frac{\partial U_L}{\partial x} + \frac{\partial V_L}{\partial y} = 0; \quad [4a]$$

the x-direction momentum is

$$0 = \frac{\partial p}{\partial x} + \frac{\partial}{\partial y}\left(\mu_L \frac{\partial U_L}{\partial y} + \tau^t_{Lxy}\right) + \rho_L g_x; \quad [4b]$$

the y-direction momentum is

$$0 = \frac{\partial p}{\partial y} + \frac{\partial}{\partial y}\tau^t_{Lyy} + \rho_L g_y; \quad [4c]$$

the Reynolds stress is

$$\tau^t_{Lxy} = -\rho_L \langle u'_L v'_L \rangle; \quad [4d]$$

and

$$\tau^t_{Lyy} = -\rho_L \langle v'_L v'_L \rangle. \quad [4e]$$

In [4a–c] time-averaged values are understood.

For fully developed conditions in the primary flow direction, which are not completely obtained in the case of evaporation and condensation, $V_L = 0$ and U_L is a function of y only. The x-direction is the primary flow direction and for flow down a vertical plate, $g_x = g$. Integrating [4b] gives

$$\mu_L \frac{dU_L}{dy} + \tau^t_{Lxy} = -\hat{p}_x y^+ + \tau_w, \quad [5a]$$

where

$$\hat{p}_x = \frac{\partial p}{\partial x} - \rho_L g \quad [5b]$$

is a constant. The dimensionless variables are

$$y^+ = \frac{yu_*}{\nu_L}, \tag{6a}$$

$$u_L^+ = \frac{U_L}{u_*}, \tag{6b}$$

$$\tau_{Lxy}^+ = \frac{\tau_{Lxy}^t}{\rho_L u_*^2}, \tag{6c}$$

$$\hat{p}_x^+ = \frac{\hat{p}_x \nu_L}{\rho_L u_*^3} \tag{6d}$$

and

$$u_* = \sqrt{\frac{\tau_w}{\rho_L}}, \tag{6e}$$

where u_* is the friction velocity based on the shear stress at the wall. With [6a–e], [5a] is

$$\frac{du^+}{dy} + \tau^+ = -\hat{p}_x^+ y^+ + 1. \tag{7}$$

Integration of [7] to obtain the velocity distribution requires the Reynolds stress τ^+ as a function of y^+, a relationship that must be obtained for each flow of interest.

The dimensionless film thickness is

$$\delta_f^+ = \frac{\delta_f u_*}{\nu_L}, \tag{8}$$

where δ_f is the film thickness, a force balance across the film gives

$$p_x^+ = \frac{(\tau_i^+ - 1)}{\delta_f^+}, \tag{9}$$

and the shear distribution in the film is

$$\tau^+(y^+) = (\tau_i^+ - 1)\left(\frac{y^+}{\delta_f^+}\right) + 1. \tag{10}$$

Models for the turbulent stresses are given in the following discussion.

2.3. Turbulent shear stress and eddy viscosity using the Prandtl mixing length

The turbulent shear stress has been modeled by many different methods for both single- and two-phase flows. Most analyses of turbulent two-phase flows use the Prandtl mixing length model and associated assumptions. The two- and three-segment empirical velocity distributions from this approach have been used by Hewitt & Hall-Taylor (1970) and others, for annular flow in a pipe. In some cases, single-phase flow models are modified to account for various aspects of two-phase flows [see Levy & Healzer (1980a–d,1981) and Abolfadal & Wallis (1985) for examples]. Some experimental investigations of separated two-phase flows have been conducted (Ueda *et al.* 1977; Davies 1972; Jeffries *et al.* 1970; Theofanous *et al.* 1976; Hanratty & Engen 1957), but results of a general nature are not available.

The Prandtl model relating shear stress to a mixing length measured from a wall and the gradient of the mean velocity is

$$\tau_{Lxy}^t = \rho_L l^2 \left|\frac{dU_L}{dy}\right| \frac{dU_L}{dy}, \tag{11a}$$

where the mixing length is

$$l = k_w y. \tag{11b}$$

In terms of the eddy viscosity for turbulent flow, the Prandtl model is

$$\nu_t = k_w^2 y^2 \left| \frac{dU_L}{dy} \right| \quad [12a]$$

and the dimensionless turbulent stress is

$$\tau^+ = k_w^2 y^{+2} \left| \frac{du^+}{dy^+} \right| \frac{du^+}{dy^+}. \quad [12b]$$

The Prandtl model has been extensively modified since its introduction by the use of damping factors, generally of the van Driest form. The simplest Prandtl model neglects damping, and breaks integration of the momentum equation into two parts; one near the wall and the second in the core region. With the standard Prandtl assumptions the velocity distribution near the wall is

$$u^+ = y^+; \quad [13a]$$

and in the fully turbulent region,

$$u^+ = \frac{1}{k_w} \ln(y^+) + B, \quad [13b]$$

Two- and three-region velocity distributions have been developed from experimental data based on the Prandtl results. The three-region model is

$$u^+ = y^+, \qquad 0 \leqslant y^+ < 5, \quad [14a]$$

$$u^+ = 5.0 \ln y^+ - 3.05, \qquad 5 \leqslant y^+ < 30, \quad [14b]$$

and

$$u^+ = 2.5 \ln y^+ + 5.5, \qquad y^+ > 30. \quad [14c]$$

The distribution of viscous dissipation per unit mass, ϵ, is

$$\epsilon(y) = \tau'_{Lxy} \frac{dU_L}{dy}; \quad [15a]$$

or in dimensionless form,

$$\epsilon^+(y^+) = \frac{du^+}{dy^+}, \quad [15b]$$

where

$$\epsilon^+(y^+) = \frac{\epsilon(y)\nu_L}{u_*^4}. \quad [15c]$$

For a film without interfacial shear, and relaxing the constant-shear assumption of the original Prandtl model, [15b] is

$$\epsilon^+(y^+) = \left(1 - \frac{y^+}{\delta_f^+}\right) \frac{du^+}{dy^+}, \quad [16]$$

where δ_f^+ is the dimensionless film thickness.

The average dissipation in the film is

$$\delta_f^+ \langle \epsilon^+(y^+) \rangle = \int_0^{\delta_f^+} \epsilon^+(y^+)\, dy^+. \quad [17]$$

Equation [17] can be integrated analytically with the velocity distribution [14a–c] and gives

$$\delta_f^+ \langle \epsilon^+(y^+) \rangle = 5.0 + 5.0 \ln(6.0) + 2.5 \ln\left(\frac{\delta_f^+}{30.0}\right) - \frac{62.5}{\delta_f^+}. \quad [18]$$

The cumulative contribution of the local dissipation to the film-average value is shown in figure 2. The results in figure 2 are obtained from [17] by quadrature. The results show that about 50% of

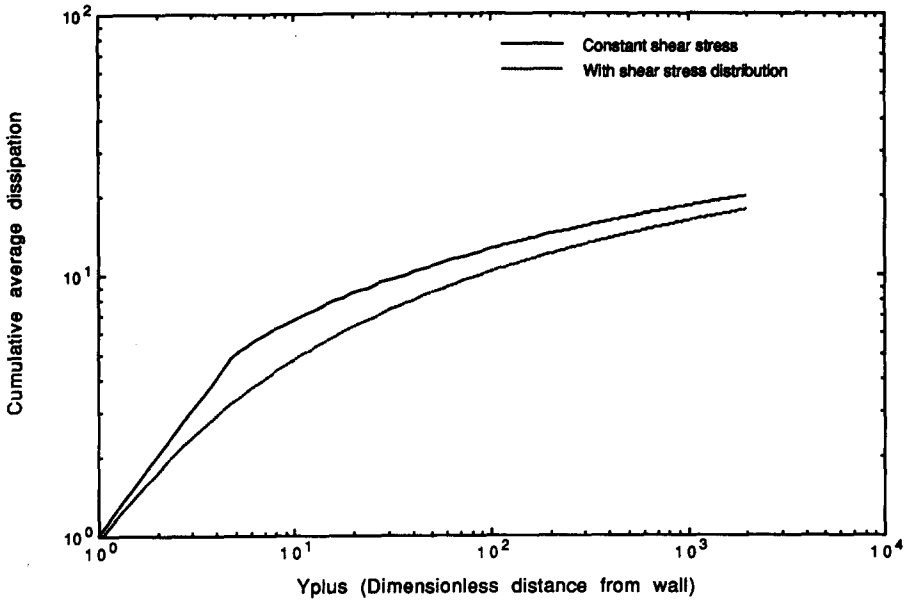

Figure 2. Cumulative normalized average dissipation for the Prandtl model with and without shear stress distribution and no interfacial shear.

the total average value is contributed by the dissipation near the wall ($y^+ < 11.6$) and that the effect of the shear stress distribution of [16] is small.

Analysis of the dissipation distribution of [18] shows that near the wall the dissipation scales as $\epsilon \sim u_*^4/\nu_L$ and in the full turbulent region $\epsilon \sim u_*^3/\delta_f$. The average dissipation also scales as u_*^3/δ_f.

We next consider a film with shear at the interface. From [10], the shear stress varies linearly,

$$\tau(y) = \tau_w\left(1 - \frac{y}{\delta_f}\right) + \tau_i \frac{y}{\delta_f}. \qquad [19]$$

The mixing length is taken as the Prandtl model or a generalization which includes damping in the wall and interface regions. A model that accounts for nonzero diffusivity at the interface is

$$l = a_l + b_l y + c_l y^2, \qquad [20a]$$

where a_l, b_l and c_l are determined from the conditions

$$l = 0 \qquad \text{at } y = 0, \qquad [20b]$$

$$\frac{dl}{dy} = k_w \qquad \text{at } y = 0, \qquad [20c]$$

$$l = k_i \delta_f \qquad \text{at } y = \delta_f. \qquad [20d]$$

These give the mixing length to be

$$l = k_w y\left[1 + \left(\frac{k_i}{k_w} - 1\right)\frac{y}{\delta_f}\right]. \qquad [21]$$

If $k_i = 0$, [21] gives a parabolic mixing length that goes to zero at an unsheared interface.

The viscous sublayer is accounted for by introduction of a van Driest damping factor into the mixing length. Again, the exact form is not so important, and we use

$$D = 1 - \exp\left(\frac{-y^+}{26}\right), \qquad [22]$$

which supplies damping in the wall region only.

With [21] and [22], the velocity distribution in a film with interfacial shear is obtained from the momentum balance of [7] as

$$u^+ = \int_0^{y^+} \frac{2\left[1+\left(\frac{\tau_i}{\tau_w}-1\right)\frac{y^+}{\delta_f}\right]dy^+}{1+\left\{1+4k_w^2y^{+2}\left[1+\left(\frac{k_i}{k_w}-1\right)\frac{y^+}{\delta_f^+}\right]^2 D^2\left[1+\left(\frac{\tau_i}{\tau_w}-1\right)\frac{y^+}{\delta_f^+}\right]\right\}^{1/2}}. \quad [23]$$

For $\tau_i = k_i = 0$ and $D = 1$, [23] reduces to the case of a film without interfacial shear with $\tau = \tau_w(1 - y/\delta_f)$. The local dissipation per unit mass is, from [16],

$$\epsilon^+(y^+) = \left[1+\left(\frac{\tau_i}{\tau_w}-1\right)\frac{y^+}{\delta_f^+}\right]\frac{du^+}{dy^+}; \quad [24]$$

and the average dissipation in the film is obtained from [17].

Some typical distributions of the turbulence properties in the film are given for three values of the ratios $\eta_\tau = \tau_i/\tau_w$ and $\eta_k = k_i/k_w$. The first case considered is for a falling film without interfacial shear ($\eta_\tau = \eta_k = 0$). The equations reduce to a mixing length that is parabolic. The velocity and cumulative average dissipation, $\delta_f^+\langle\epsilon^+(y^+)\rangle$, are shown in figures 3a and 3b, respectively.

The second case is a sheared film with $\eta_\tau = 0.10$ and $\eta_k = 0.0$, which represents a small interfacial shear with the eddy viscosity damped at the interface. The velocity and cumulative dissipation are given in figures 4a and 4b, respectively. The final case is a sheared film with $\eta_\tau = 1.0$ and $\eta_k = 1.0$, and these results are shown in figures 5a and 5b, respectively.

The results in figures 3–5, indicate: firstly, the velocity distribution is not greatly affected by the details of the mixing length and shear stress distributions; and secondly, the average dissipation is dominated by the wall region. About 50% of the average dissipation occurs for $y^+ \lesssim 11.6$.

The velocity distribution in figures 3a and 4a indicates an increase in the velocity near the interface; a characteristic shown in the data of Ueda *et al.* (1977) for an open channel flow. These authors noted that measurement of the surface velocity by a floating particle method indicated that the surface velocity was about 4% higher than would be predicted by the logarithmic distribution of [13b]. Tsanis (1989) has also observed this characteristic for the surface velocity of oceans and flumes. This trend is captured by the film flow model with a parabolic mixing length.

2.4. Dissipation and the renewal period

The results of the previous section provide information about incorporating the dissipation into the renewal period $t_{rp} = (\nu_L/\epsilon)^{1/2}$. The surface renewal expression for heat and mass transfer coefficients requires $(1/t_{rp})^{1/2} = (\epsilon/\nu_L)^{1/4}$, and this form is convenient for the following discussion. The results in the previous section have shown the following: near the wall, the dissipation scales as u_*^4/ν_L; the viscous sublayer and transition region provide about 50% of the average dissipation; and the fully turbulent and the average dissipation scale as u_*^3/δ_f.

These results suggest the following integral measures of the dissipation in a film:

1. A value based on the average of the wall and interfacial shear $\tau_c = (\tau_w + \tau_i)/2$. Hughmark (1973) has previously proposed this value, and Henstock & Hanratty (1979) have used $\tau_c = (2/3)\tau_w + (1/3)\tau_i$.
2. For $\tau_i = 0$, or small relative to τ_w, dissipation based upon the wall value may be used.

The dimensionless dissipation in the wall region is (see [15]):

$$\epsilon^+ = 1 \quad [25a]$$

or

$$\epsilon = \frac{u_*^4}{\nu_L}. \quad [25b]$$

Using the average shear stress as the characteristic stress, scaling with the wall region given the dissipation as

$$\epsilon = \left(\frac{1}{4\rho_L^2 \nu_L}\right)(\tau_w + \tau_i)^2. \qquad [26]$$

Correlations for the wall and interface friction factors in τ_w and τ_i are given in the appendix.

3. APPLICATIONS AND DATA COMPARISONS

In the following discussion, the results of the analyses in the previous section are applied to falling films with heat transfer, evaporation and condensation, and to condensation onto horizontal liquid films.

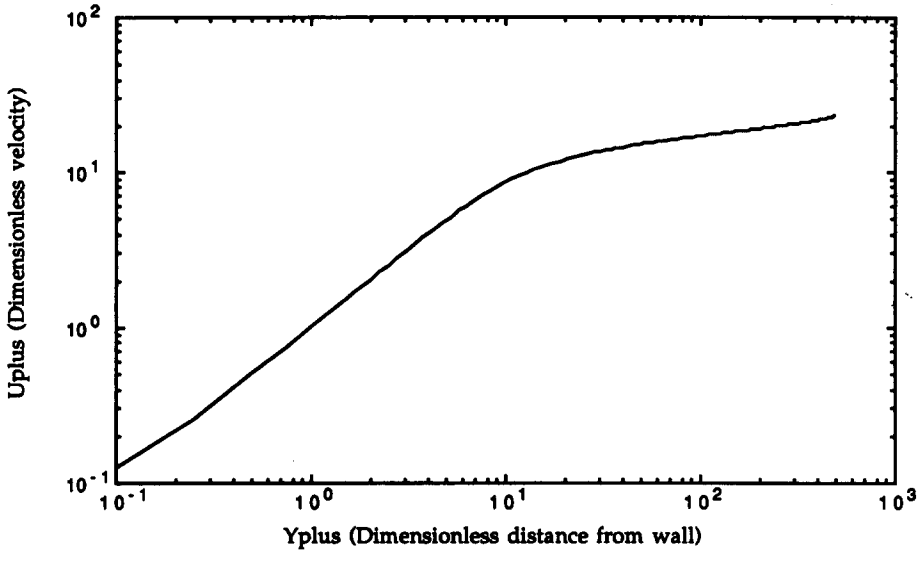

Figure 3a. Velocity distribution in an unsheared film with parabolic mixing length.

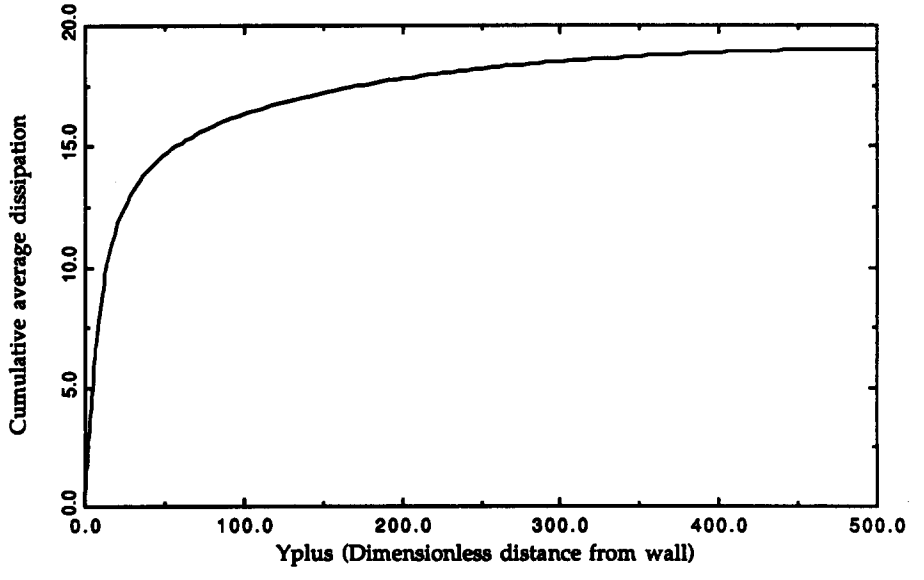

Figure 3b. Cumulative average dissipation in an unsheared film with parabolic mixing length.

3.1. *Falling liquid films*

The surface renewal model developed in the previous sections cannot distinguish between heating of a subcooled film, evaporation of a saturated film by a heated surface or condensation of a liquid onto a solid surface. Experimental data and analyses have lead to correlations of the Nusselt number, Nu, as a function of the film Reynolds number, Re, and liquid Prandtl number, Pr, for heating, in the form

$$\mathrm{Nu} = \frac{h\nu_L^{2/3}}{k_L g^{1/3}} = C_h \mathrm{Re}^m \mathrm{Pr}^n. \qquad [27]$$

The most recent value of the exponents are $m = 0.3$ and $n = 0.6$ (Shmerler & Mudawwar 1988a). Other values have been reported and range from 0.16 to 0.40 for m and from 0.50 to 0.63 for n, for heating, and up to 0.95 for evaporation (Shmerler & Mudawwar 1988b).

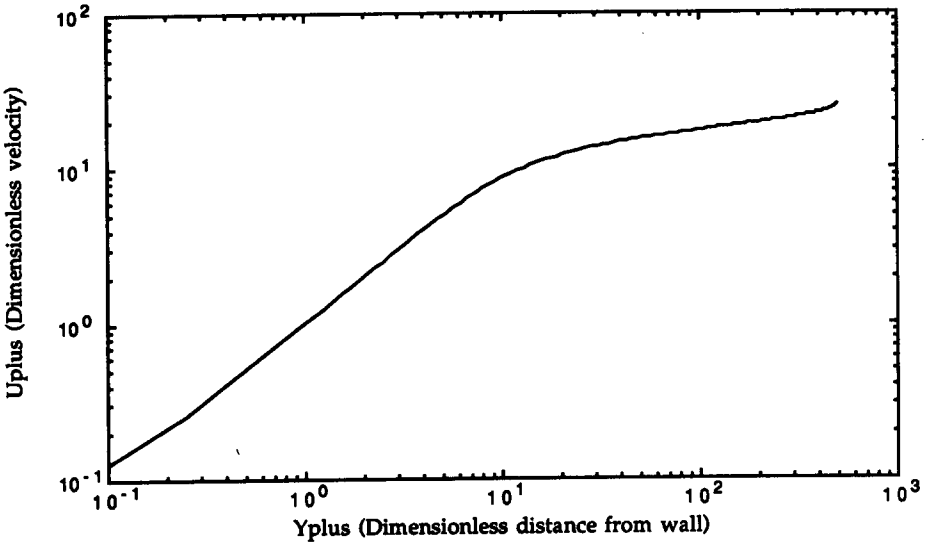

Figure 4a. Velocity distribution in a sheared film with parabolic mixing length with $\tau_i/\tau_w = 0.10$.

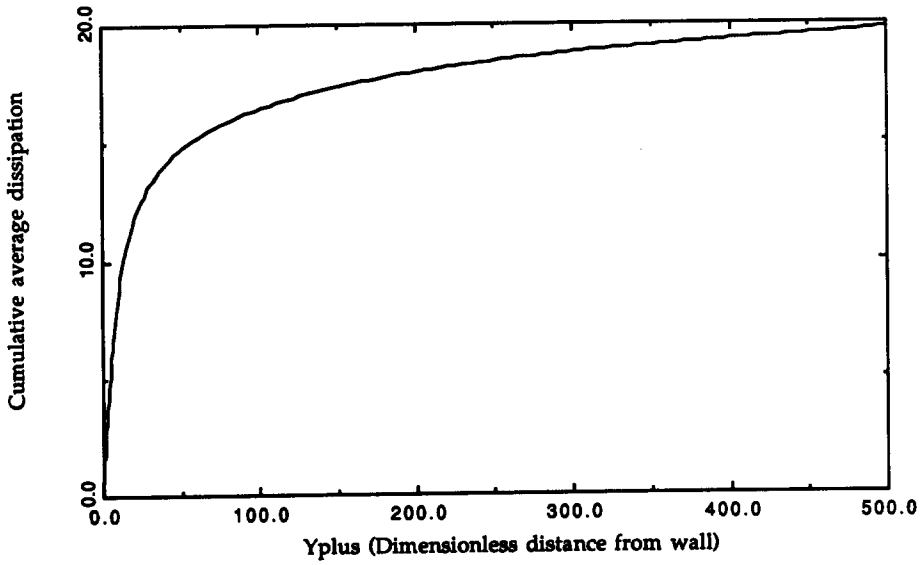

Figure 4b. Cumulative average dissipation in a sheared film with parabolic mixing length with $\tau_i/\tau_w = 0.10$.

For a film without interfacial shear, the wall shear is

$$\tau_w = \rho_L \delta_f g \cos\theta; \qquad [28a]$$

the shear velocity is

$$u_* = (\delta_f g \cos\theta)^{1/2}; \qquad [28b]$$

the dissipation from [26] is

$$\epsilon = \frac{(\delta_f^2 g^2 \cos^2\theta)}{\nu_L}; \qquad [28c]$$

and the square root of the reciprocal of the renewal period is

$$\left(\frac{1}{t_{rp}}\right)^{1/2} = \left(\frac{\epsilon}{\nu_L}\right)^{1/4} = \left(\frac{\delta_f g \cos\theta}{\nu_L}\right)^{1/2}. \qquad [28d]$$

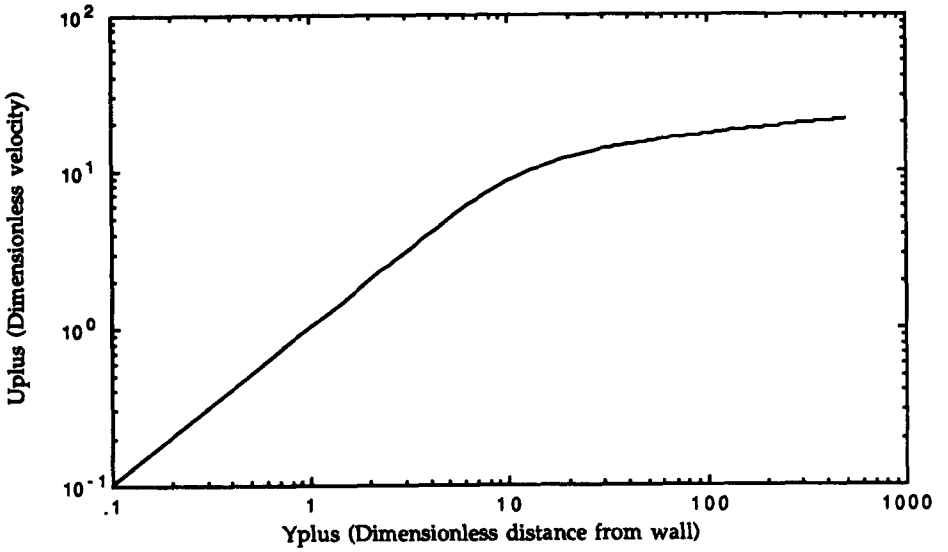

Figure 5a. Velocity distribution in a sheared film with Prandtl mixing length with $\tau_i/\tau_w = 1.00$ and $k_i/k_w = 1.00$.

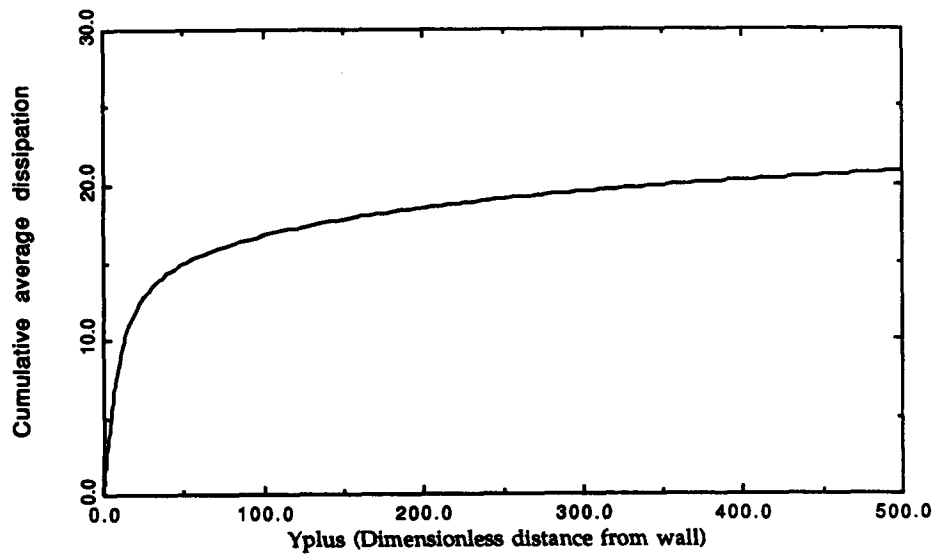

Figure 5b. Cumulative average dissipation in a sheared film with Prandtl mixing length with $\tau_i/\tau_w = 1.00$ and $k_i/k_w = 1.00$.

Equation [28d] is a form of the Carpenter–Colburn analogy between momentum and heat transfer.

With [28d], the heat transfer coefficient from the renewal model is

$$h_h = 2\rho_L c_{pL}\sqrt{\frac{\alpha_{tL}}{\pi}}\left(\frac{\delta_f g}{\nu_L}\right)^{1/2}. \quad [29]$$

Rearranging [29] to dimensionless form gives

$$\mathrm{Nu} = \frac{h\nu_L^{2/3}}{k_L g^{1/3}} \sim \mathrm{Re}^{m_{\delta_f}/2}\mathrm{Pr}^{1/2}, \quad [30]$$

where m_{δ_f} is the exponent in the film thickness–Re relationship. These correlations are in the form

$$\delta_f = \frac{\delta_f g^{1/3}}{\nu_L^{2/3}} = C_{\delta_f}\mathrm{Re}^{m_{\delta_f}}. \quad [31]$$

Several correlations are available and the exponent m_{δ_f} varies from about 0.5 to 0.67. Equation [30] thus predicts the heat transfer coefficient will depend on Re to a power between 0.25 and 0.33; in line with analytical and experimental studies. The surface renewal theory predicts that the Pr-dependence will be 1/2.

We make the following observations. First, the renewal theory cannot distinguish between heating, evaporation and condensation for falling films. Thus, the dependencies given above will hold for all three processes.

Secondly, the corresponding development of the mass transfer problem for gas absorption at the interface will give the same dependency on Re. The result is not consistent with the corresponding experimental data. Theofanous (1984) and others show that the mass transfer coefficient increases much faster with Re than the value obtained here. This is because processes *at the interface* dominate.

For a falling film with interfacial shear, the analysis proceeds by use of [26] for the dissipation. Putting [26] into [28d] for the renewal time period and that result into [3] for the heat transfer coefficient gives

$$h_c = 2\rho_L c_{pL}\sqrt{\frac{\alpha_{tL}}{\pi}}\left(\frac{1}{4\rho_L^2\nu_L^2}\right)^{1/4}(\tau_w + \tau_i)^{1/2}, \quad [32a]$$

which for a falling film and with introduction of dimensionless variables becomes

$$\mathrm{Nu} = \frac{h\nu_L^{2/3}}{k_L g^{1/3}} \sim (\delta_f^+\,\mathrm{Pr} + \tau_i^*\mathrm{Pr})^{1/2}, \quad [32b]$$

where the dimensionless film thickness is given by [31], or obtained from the flow model.

Chen *et al.* (1987) report the effect of interfacial shear is to modify the heat transfer, increasing it for cocurrent flow and decreasing for countercurrent. The latter authors suggested adding together, in quadrature, the laminar, turbulent and shear contributions, via their [8] for the local Nu:

$$\mathrm{Nu} = \frac{h}{k_L}\left(\frac{\nu_L^2}{g}\right)^{1/3} = \left[\left(0.31\,\mathrm{Re}^{-1.32} + \frac{\mathrm{Re}^{2.4}\mathrm{Pr}^{3.9}}{2.317\cdot 10^{14}}\right)^{1/3} + \frac{\mathrm{Pr}^{1/3}}{771.6}\tau_i^*\right]^{1/2}, \quad [33a]$$

where $\tau_i^* = \tau_i/\rho_L(g\nu_L)^{2/3}$, the nondimensional shear stress. Chen *et al.* further stated that a constant shear stress could be assumed, or the interfacial shear taken as the wall value.

The average Nu is

$$\overline{\mathrm{Nu}} = \left(\mathrm{Re}^{-0.44} + \frac{\mathrm{Re}^{0.8}\mathrm{Pr}^{1.3}}{1.718\cdot 10^5} \pm \frac{\mathrm{Pr}^{1.3}}{771.6}\tau_i^*\right)^{1/2}, \quad [33b]$$

where the positive sign is for cocurrent flow. These results fit data well, although the range of Re is limited (i.e. Re < 5000). In the high shear limit, the last term dominates and the condensation or evaporation rate will increase as $(\tau_i^*)^{1/2}$.

The form of our theoretical results, [32a,b], is in agreement with the turbulent terms in the Chen *et al.* (1987) correlation, [33b]. Their correlation has exponents on Re and Pr of 0.80 and 1.30, respectively when written in the form of [32b]. (In [32b], the exponent on Re will have the value that is in the film thickness.) Hubbard *et al.* (1976) have also shown that the heat transfer coefficient for films with interfacial shear depends linearly on the shear. We do not repeat the extensive comparisons available in these papers with falling film data.

3.2. Mass transfer and interfacial shear in liquid films

With the present theory, we have shown that the form of the heat transfer coefficient is given by [32b]. The analogy between heat and mass transfer gives the equivalent expression for the Sherwood number as

$$\mathrm{Sh} = \frac{k_L D_e}{D_m} \sim (\delta_f^+ \mathrm{Sc} + \tau_i^* \mathrm{Sc})^{1/2}, \qquad [34a]$$

where k_L is the mass transfer coefficient, D_e is a characteristic dimension, D_m is the mass diffusivity and Sc is the Schmidt number. Equation [34a] can be written as

$$\frac{\mathrm{Sh}}{\mathrm{Sh}_0} = \left(1 + \frac{\tau_i^*}{\mathrm{Re}^{m_{\delta_f}}}\right)^{1/2}, \qquad [34b]$$

where Sh_0 is the value of the Sherwood number for zero interfacial shear, which is not given by our theory. Utilizing the relationship between film thickness and Re, we write

$$\mathrm{Re}^{m_{\delta_f}} \sim \frac{\tau_{w0}}{\rho_L g^{1/2} \nu_L}, \qquad [34c]$$

where τ_{w0} is the wall shear stress $\rho_L g \delta_f$. Expanding [34b] by the binomial theorem and substituting the film thickness correlation, gives

$$\frac{\mathrm{Sh}}{\mathrm{Sh}_0} = 1 + a\left(\frac{\tau_i}{\tau_{w0}}\right), \qquad [34d]$$

where a is a constant of proportionality. This result is *identical in form* to that obtained by Chung & Mills (1974) by empirical correlation of film flow gas absorption data. Thus, the present theory is entirely consistent with the data. We expect nonlinear effects for large values of (τ_i/τ_{w0}), but data are not available to check this at present.

3.3. Condensation of a vapor onto its liquid in horizontal flow

The theory is next applied to condensation of vapor onto subcooled liquid in a horizontal stratified flow, where the depth is larger than in a film and the wall shear is significant. Experimental data have been given in a series of reports by Cook *et al.* (1981), Lim *et al.* (1981,1984), Lee *et al.* (1979), Lee (1985), Bankoff *et al.* (1981,1982), Bankoff & Kim (1985), Kim & Bankoff (1983), Kim (1985) and Jensen & Yuen (1982). These reports contain data and analysis of condensation of steam onto subcooled water for both cocurrent and countercurrent, vertical and horizontal flow. The specific data used here are reported by Lim *et al.* (1981,1984) for cocurrent horizontal stratified flow in a rectangular channel. The channel was 1.601 m long, 0.305 m wide and 0.0640 m high. The local rate of condensation predicted by theory can be compared with measurements. These data cover wide ranges of operating parameters for liquid temperature and initial vapor and liquid flow rates, as summarized in table 1.

As shown in table 1, the experiments systematically covered the effects of liquid and vapor inlet flow at two values of the liquid inlet temperature. The liquid Re values ranged from about 10,000 to about 50,000, and are larger than those encountered in falling film experiments. The heat transfer coefficient between the vapor and liquid ranged from about 2 to about 25 kW/m^2 K.

The flow is constantly developing in the primary flow direction: the liquid film thickness and temperature increase and the vapor velocity decreases, due to condensation. Variations in the flow are calculated by a standard one-dimensional flow model given in the appendix.

The dissipation for the renewal period in the heat transfer coefficient was calculated by [26] using the interfacial friction factors given in the appendix. This model is exactly equivalent to the

Table 1. Summary of the operating ranges for the Lim *et al.* (1981) experimental data

Run series No.	Liquid inlet temperature (K)	Liquid inlet mass flow rate (kg/s)	Vapour inlet mass flow rate (kg/s)
25×	298.0	0.65	0.065, 0.093, 0.125, 0.16
27×	298.0	1.03	0.065, 0.093, 0.125. 0.16
29×	298.0	1.44	0.065, 0.90, 0.126
35×	298.0	0.68	0.066, 0.1242
37×	298.0	1.02	0.064, 0.124
39×	298.0	1.42	0.064, 0.126
45×	323.0	0.70	0.065, 0.094, 0.130, 0.16
47×	323.0	1.06	0.064, 0.090, 0.130, 0.16
49×	323.0	1.40	0.065, 0.091, 0.130

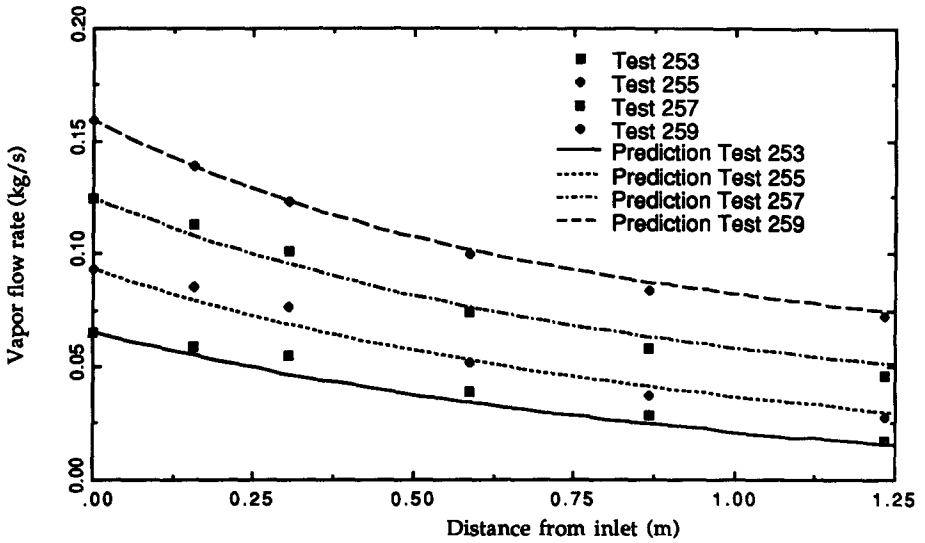

Figure 6a. Prediction of Lim *et al.* series 25× data using the characteristic shear stress and the Blasius correlation for wall friction and the Eck correlation for interface friction (liquid inlet flow = 0.65 kg/s; inlet temperature = 298.0 K).

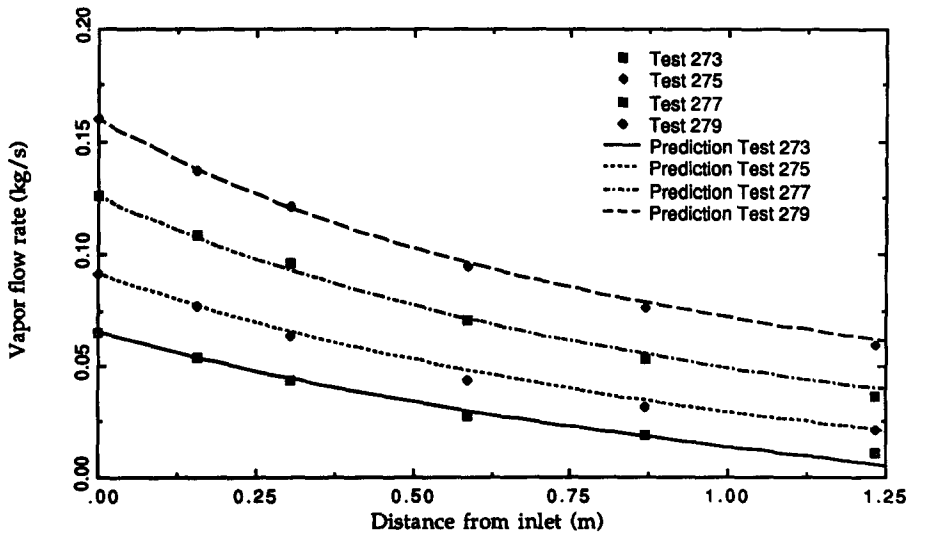

Figure 6b. Prediction of Lim *et al.* series 27× data using the characteristic shear stress and the Blasius correlation for wall friction and the Eck correlation for interface friction (liquid inlet flow = 1.03 kg/s; inlet temperature = 298.0 K).

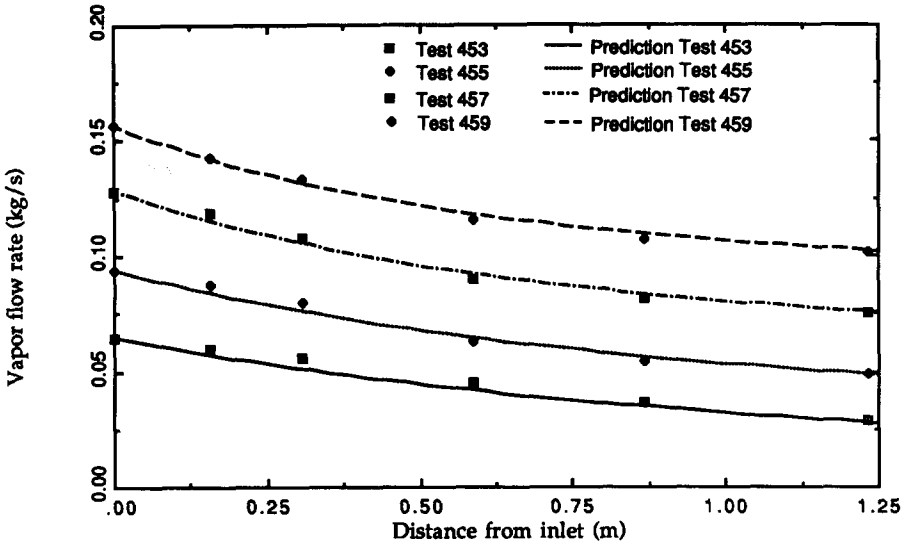

Figure 6c. Prediction of Lim *et al.* series 45× data using the characteristic shear stress and the Blasius correlation for wall friction and the Eck correlation for interface friction (liquid inlet flow = 0.70 kg/s; inlet temperature = 323.0 K).

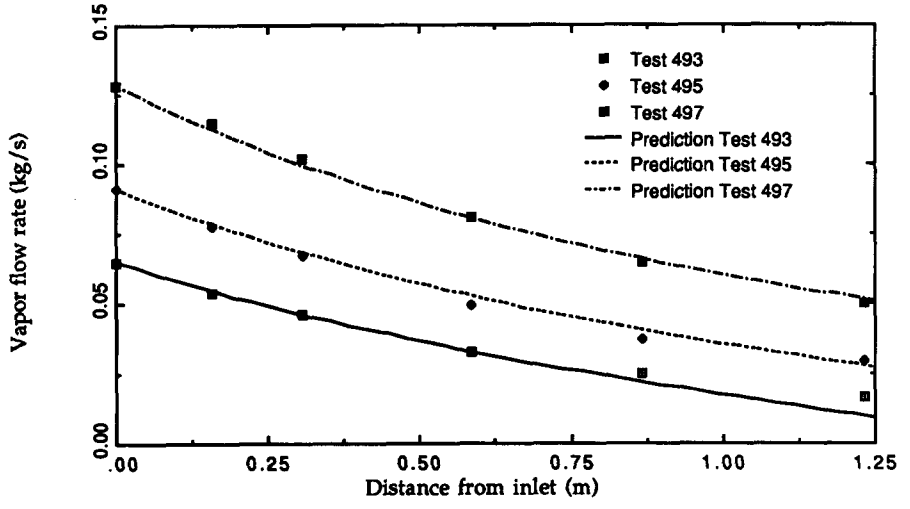

Figure 6d. Prediction of Lim *et al.* series 49× data using the characteristic shear stress and the Blasius correlation for wall friction and the Eck correlation for interface friction (liquid inlet flow = 1.40 kg/s; inlet temperature = 323.0 K).

model used to obtain the form of the Chen *et al.* (1987) correlation, [32b], above. In the present application however, the complete system of equations determines the coefficients that would appear in an empirical correlation.

The results of predictions of some of the experimental data are given in figures 6 and 7, for the Eck and Andritsos & Hanratty friction correlations, respectively. The agreement of the model predictions with the data is excellent. The variation in heat transfer along the channel causes the slope of the vapor flow rate to change, and the predictions follow this with good accuracy. The theory tends to predict condensation rates that are larger than experimental values for lower vapor flow rates. Other than this characteristic, the theory predicts both the magnitude and functional dependencies of the vapor condensation rate. All the data summarized in table 1 have been predicted. The comparisons not reported here are equally as good as those shown in the figures. The results of calculations using other models for the dissipation were not as successful as those reported here.

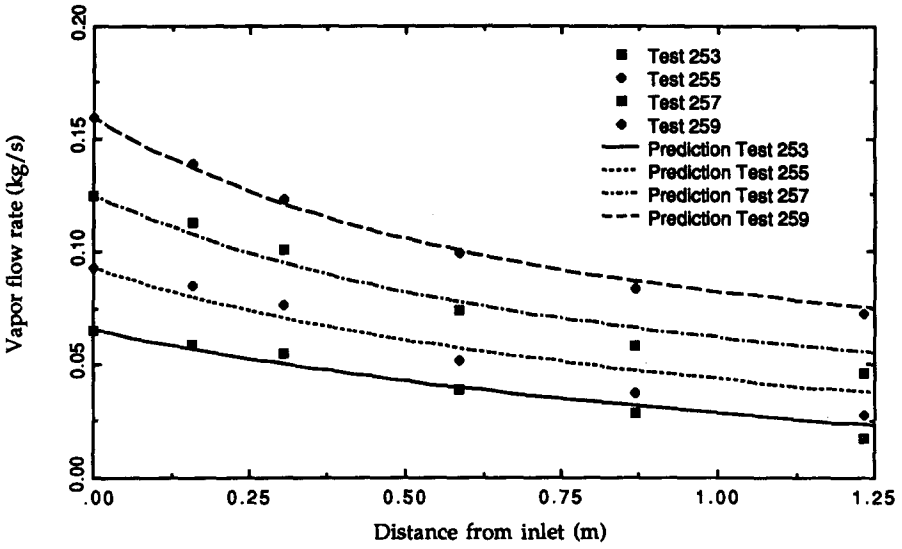

Figure 7a. Prediction of Lim *et al.* series 25× data using the characteristic shear stress and the Blasius correlation for wall friction and the Andritsos & Hanratty correlation for interface friction (liquid inlet flow = 0.65 kg/s; inlet temperature = 298.0 K).

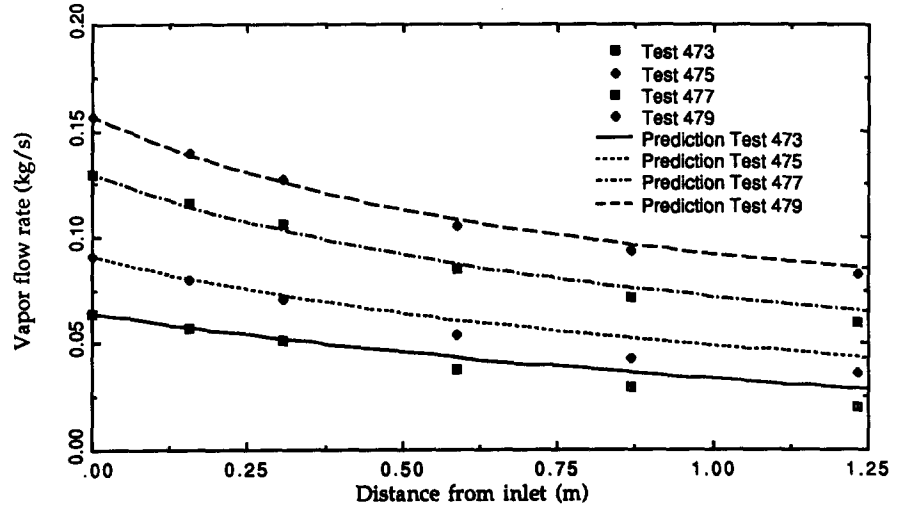

Figure 7b. Prediction of Lim *et al.* series 47× data using the characteristic shear stress and the Blasius correlation for wall friction and the Andritsos & Hanratty correlation for interface friction (liquid inlet flow = 1.06 kg/s; inlet temperature = 323.0 K).

4. SUMMARY AND CONCLUSIONS

Investigations into the turbulence characteristics of the liquid film in separated two-phase flows, and application of surface renewal theory to these flows have led to: (1) theoretical predictions; and (2) accurate comparisons with data. The results are obtained using Kolmogorov length and velocity scales, based on a characteristic average shear stress for the film, for the renewal period in the surface renewal theory. The dissipation in the liquid film is governed by contributions from both the wall and the interface shear stress. The theoretical predictions are in agreement with the form of heat and mass transfer coefficient correlations and experimental data including the effect of interfacial shear.

Comparisons with experimental data for condensation of water vapor onto subcooled liquid water indicate that the theory predicts both the magnitude and the functional dependencies of the condensation process with excellent accuracy. The theoretical approach is also applicable to other heat and mass transfer problems.

Acknowledgement—This research was supported by the U.S. Department of Energy Idaho Operations Office under Contract No. DE-AC07-76ID01570.

REFERENCES

ABOLFADAL, M. & WALLIS, G. B. 1985 A mixing length model for annular two-phase flow. *PhysicoChem. Hydrodynam.* **6,** 49–68.

ANDREUSSI, P., ASALI, J. C. & HANRATTY, T. J. 1985 Initiation of roll waves in gas–liquid flows. *AIChE Jl* **31,** 119–126.

ANDRITSOS, N. & HANRATTY, T. J. 1987a Influence of interfacial waves in stratified gas–liquid flows. *AIChE Jl* **33,** 444–454.

ANDRITSOS, N. & HANRATTY, T. J. 1987b Interfacial instabilities for horizontal gas–liquid flows in pipelines. *Int. J. Multiphase Flow* **13,** 583–603.

ASALI, J. C., HANRATTY, T. J. & ANDREUSSI, P. 1985 Interfacial drag and film height for vertical annular flow. *AIChE Jl* **31,** 895–902.

BANERJEE, S. 1978 A surface renewal model for interfacial heat and mass transfer in transient two-phase flow. *Int. J. Multiphase Flow* **4,** 571–573.

BANERJEE, S., SCOTT, D. S. & RHODES, E. 1968 Mass transfer to falling wavy liquid films in turbulent flow. *Ind. Engng Chem. Fundam.* **7,** 22–26.

BANKOFF, S. G. & KIM, H. J. 1985 Direct-contact condensation of steam on cold water in stratified countercurrent flow. USNRC Report NUREG/CR-4414.

BANKOFF, S. G., TANKIN, R. S. & YUEN, M. C. 1981 Steam–water condensation studies. USNRC Report NUREG/CR-1898.

BANKOFF, S. G., KIM, H. J., TANKIN, R. S. & YUEN, M. C. 1982 Countercurrent steam–water flow in a flat plate geometry. USNRC Report NUREG/CR-2783.

BERRY M. R. JR & GOSS, W. P. 1972 An integral analysis of condensing annular–mist flow. *AIChE Jl* **18,** 754–761.

BRUMFIELD, L. K. & THEOFANOUS, T. G. 1976 Turbulent mass transfer in jet flow and bubble flow: a reappraisal of Levich's theory. *AIChE Jl* **22,** 607–610.

BRUMFIELD, L. K., HOUZE, R. N. & THEOFANOUS, T. G. 1975 Turbulent mass transfer at free, gas–liquid interfaces, with application to film flows. *Int. J. Heat Mass Transfer* **8,** 1077–1081.

CHEN, S. L., GERNER, F. M. & TIEN, C. L. 1987 General film condensation correlations. *Expts Heat Transfer* **1,** 93–107.

CHEREMISINOFF, N. P. & DAVIS, E. J. 1979 Stratified turbulent–turbulent gas–liquid flow. *AIChE Jl* **25,** 48–53.

CHUNG, D. K. & MILLS, A. F. 1974 Effect of interfacial shear on gas absorption into a turbulent falling film co-current gas flow. *Lett. Heat Mass Transfer* **1,** 43–48.

CHUNG, D. K. & MILLS, A. F. 1976 Experimental study of gas absorption into turbulent falling films of water and ethylene glycol–water mixtures. *Int. J. Heat Mass Transfer* **19,** 51–59.

COOK, D., BANKOFF, S. G., TANKIN, R. S. & YUEN, M. C. 1981 Countercurrent steam–water flow in a vertical channel. USNRC Report NUREG/CR-2056.

DAVIES, J. T. 1972 Turbulence phenomena at free surfaces. *AIChE Jl* **18,** 169–173.

DAVIES, J. T. & HAMEED, A. 1971 Gas absorption into turbulent jets of kerosene. *Chem. Engng Sci.* **26,** 1295–1296.

DAVIES, J. T. & TING, S. T. 1967 Mass transfer into turbulent jets. *Chem. Engng Sci.* **22,** 1537–1548.

DAVIES, J. T. & WARNER, K. V. 1969 The effect of large-scale roughness in promoting gas absorption. *Chem. Engng Sci.* **24,** 231–240.

DUFFEY, R. B. & HUGHES, E. D. 1991 CO_2 and gas mass transfer across ocean, lake and river surfaces: a constitutive law. *J. geophys. Res.* Submitted.

FORTESCUE, G. E. & PEARSON, J. R. A. 1967 On gas absorption into a turbulent liquid. *Chem. Engng Sci.* **22,** 1163–1176.

HAMERSMA, P. J. & HART, J. 1987 A pressure drop correlation for gas/liquid pipe flow with a small liquid holdup. *Chem. Engng Sci.* **42,** 1187–1196.

HANRATTY, T. J. & ENGEN, J. M. 1957 Interaction between a turbulent air stream and a moving water surface. *AIChE Jl* **3,** 299–304.

HART, J., HAMERSMA, P. J. & FORTUIN, J. M. H. 1989 Correlations predicting frictional pressure drop and liquid holdup during horizontal gas–liquid flow with a small liquid holdup. *Int. J. Multiphase Flow* **15,** 947–964.

HENSTOCK, W. H. & HANRATTY, T. J. 1979 Gas absorption by a liquid layer flowing on the wall of a pipe. *AIChE Jl* **25,** 122–131.

HEWITT, G. F. & HALL-TAYLOR, N. S. 1970 *Annular Two-phase Flow.* Pergamon Press, Oxford.

HIDY, G. M. & PLATE, E. J. 1966 Wind action on water standing in a laboratory channel. *J. Fluid Mech.* **26,** 651–687.

HIGBIE, R. 1935 The rate of absorption of a pure gas into a still liquid during short periods of exposure. *AIChE Jl* **31,** 365–389.

HUBBARD, G. L., MILLS, A. F. & CHUNG, D. K. 1976 Heat transfer across a turbulent falling film with cocurrent vapor flow. *J. Heat Transfer* **98,** 319–320.

HUGHMARK, G. A. 1973 Film thickness, entrainment, and pressure drop in upward annular and dispersed flow. *AIChE Jl* **19,** 1021–1056.

JEFFRIES, R. B., SCOTT, D. S. & RHODES, E. 1970 Structure of turbulence close to the interface in the liquid phase of a co-current stratified two-phase flow. *Proc. Instn Mech. Engrs* **184,** 204–214.

JENSEN, R. J. & YUEN, M. C. 1982 Interphase transport in horizontal stratified concurrent flow. USNRC Report NUREG/CR-2334.

JEPSEN, J. C., CROSSER, O. K. & PERRY, R. H. 1966 The effect of wave induced turbulence on the rate of absorption of gases in falling liquid films. *AIChE Jl* **12,** 186–192.

KIM, H. J. 1985 Local properties of countercurrent stratified steam–water flow. USNRC Report NUREG/CR-4417.

KIM, H. J. & BANKOFF, S. G. 1983 Local heat transfer-coefficients for condensation in stratified countercurrent steam–water. *J. Heat Transfer* **105,** 706–712.

KOUTITAS, C. & O'CONNOR, B. 1980 Modeling three-dimensional wind-induced flows. *J. Hydraul. Div. Proc. ASCE* **106,** 1843–1865.

LAMONT, J. C. & SCOTT, D. S. 1970 An eddy cell model of mass transfer into the surface of a turbulent liquid. *AIChE Jl* **16,** 513–519.

LAMOURELLE, A. P. & SANDALL, O. C. 1972 Gas absorption into a turbulent liquid. *Chem. Engng Sci.* **27,** 1035–1043.

LANDAHL, M. T. & MOLLO-CHRISTENSEN, E. 1986 *Turbulence and Random Processes in Fluid Mechanics.* Cambridge Univ. Press, Cambs.

LEE , L., BANKOFF, S. G., YUEN, M. C., JENSEN, R. & TANKIN, R. S. 1979 Local condensation rates in horizontal cocurrent steam–water flow. In *Nonequilibrium Interfacial Transport Processes,* pp. 79–83. ASME, New York.

LEE, S. C. 1985 Stability of steam–water countercurrent stratified flow. USNRC Report NUREG/CR-4416.

LEVICH, V. G. 1962 *Physicochemical Hydrodynamics.* Prentice-Hall, Englewood Cliffs, N.J.

LEVY, S. & HEALZER, J. M. 1980a Prediction of annular liquid–gas flow with entrainment—cocurrent vertical pipe flow with no gravity. Electric Power Research Inst. Report EPRI NP-1409.

LEVY, S. & HEALZER, J. M. 1980b Prediction of annular liquid–gas flow with entrainment—cocurrent vertical pipe flow with gravity. Electric Power Research Inst. Report EPRI NP-1521.

LEVY, S. & HEALZER, J. M. 1980c Analysis of annular liquid–gas flow with entrainment—cocurrent vertical flow in an annulus. Electric Power Research Inst. Report EPRI NP-1563.

LEVY, S. & HEALZER, J. M. 1980d Prediction of critical heat flux for annular flow in vertical pipes. Electric Power Research Inst. Report EPRI NP-1619.

LEVY, S. & HEALZER, J. M. 1981 Application of mixing length theory to wavy turbulent liquid–gas interface. *J. Heat Transfer* **103,** 492–500.

LIM, I. S., BANKOFF, S. G., TANKIN, R. S. & YUEN, M. C. 1981 Cocurrent steam/water flow in a horizontal channel. USNRC Report NUREG/CR-2289.

LIM, I. S., TANKIN, R. S. & YUEN, M. C. 1984 Condensation measurement of horizontal cocurrent steam/water flow. *J. Heat Transfer* **106,** 425–432.

LIMBERG, H. 1973 Warmeubergang An Turbulente Und Laminare Rieselfilme. *Int. J. Heat Mass Transfer* **16,** 1691–1702.

MILLS, A. F. & CHUNG, D. K. 1973 Heat transfer across turbulent falling films. *Int. J. Heat Mass Transfer* **16,** 694–696.

MOECK, E. O. 1970 Annular–dispersed two-phase flow and critical heat flux. Report AECL-3656.

MUDAWWAR, I. A. & EL-MASRI, M. A. 1986 Momentum and heat transfer across freely-falling turbulent liquid films. *Int. J. Multiphase Flow* **12,** 771–790.

RASTOGI, A. K. & RODI, W. 1978 Predictions of heat and mass transfer in open channels. *J. Hydraul. Div. Proc. ASCE* **104,** 397–420.

SCHLICHTING, H. 1979 *Boundary-layer Theory.* McGraw-Hill, New York.

SEBAN, R. A. & FAGHRI, A. 1976 Evaporation and heating with turbulent falling liquid films. *J. Heat Transfer* **98,** 315–331.

SHMERLER, J. A. & MUDAWWAR, I. 1988a Local heat transfer coefficient in wavy free-falling turbulent liquid films undergoing uniform sensible heating. *Int. J. Heat Mass Transfer* **31,** 67–77.

SHMERLER, J. A. & MUDAWWAR, I. 1988b Local evaporative heat transfer coefficient in turbulent free-falling liquid films. *Int. J. Heat Mass Transfer* **31,** 731–742.

THEOFANOUS, T. G. 1984 Conceptual models of gas exchange. In *Gas Transfer at Water Surfaces* (Edited by BRUTSAERT, W. & JIRKA, H.), pp. 271–281. Reidel, Dordrecht, The Netherlands.

THEOFANOUS, T. G., HOUZE, R. N. & BRUMFIELD, L. K. 1976 Turbulent mass transfer at free, gas–liquid interfaces, with application to open-channel, bubble and jet flows. *Int. J. Multiphase Flow* **2,** 613–624.

TSANIS, I. 1989 Simulation of wind-induced water currents. *J. Hydraul. Engng* **115,** 1113–1134.

UEDA, H., MOLLER, R., KOMORI, S. & MIZUSHINA, T. 1977 Eddy diffusivity near the free surface of open channel flow. *Int. J. Heat Mass Transfer* **20,** 1127–1136.

WALLIS, G. B. 1969 *One-dimensional Two-phase Flow.* McGraw-Hill, New York.

WON, Y. S. & MILLS, A. F. 1982 Correlation of viscosity and surface tension on gas absorption into freely falling turbulent liquid films. *Int. J. Heat Mass Transfer* **25,** 223–229.

APPENDIX

One-dimensional Flow Equations

The continuity equation for the liquid is

$$\frac{\mathrm{d}}{\mathrm{d}x} W_{\mathrm{L}} = \dot{m}_{\mathrm{GL}} \bar{A}_{\mathrm{GL}} A_{\mathrm{f}}; \qquad \text{[A.1a]}$$

for the vapor,

$$\frac{\mathrm{d}}{\mathrm{d}x} W_{\mathrm{G}} = -\dot{m}_{\mathrm{GL}} \bar{A}_{\mathrm{GL}} A_{\mathrm{f}}; \qquad \text{[A.1b]}$$

and for the mixture, $W = W_{\mathrm{G}} + W_{\mathrm{L}}$; where W_{L}, W_{G} and W are the mass flow rate of the liquid, vapor and mixture, respectively, m_{GL} is the mass exchange flux, A_{GL} is the interfacial area per unit fluid volume and A_{f} is the channel flow area.

The energy equation for the liquid is

$$W_{\mathrm{L}} c_{\mathrm{pL}} \frac{\mathrm{d}}{\mathrm{d}x} T_{\mathrm{L}} = q_{\mathrm{iGL}} \bar{A}_{\mathrm{GL}} A_{\mathrm{f}}, \qquad \text{[A.2a]}$$

where T_{L} is the liquid temperature and q_{iGL} is the heat flux at the interface. The heat flux is given by surface renewal theory, [2a] in the text, and the mass exchange is

$$\dot{m}_{\mathrm{GL}} = \frac{q_{\mathrm{iGL}}}{(h_{\mathrm{Gs}} - h_{\mathrm{L}})}, \qquad \text{[A.2b]}$$

where h_{Gs} and h_{L} are the vapor and liquid enthalpy, respectively. The pressure gradient in the liquid film is

$$\frac{\mathrm{d}p}{\mathrm{d}x} = -\bar{A}_{\mathrm{wL}} B_{\mathrm{wL}} U_{\mathrm{L}} - \bar{A}_{\mathrm{GL}} B_{\mathrm{GL}} (U_{\mathrm{G}} - U_{\mathrm{L}}), \qquad \text{[A.3a]}$$

where U_L and U_G are the mean velocity of the liquid and vapor, respectively, and the shear stress coefficients are

$$B_{wL} = \tfrac{1}{8}\rho_L f_{wL}|U_L| \qquad [A.3b]$$

and

$$B_{GL} = \tfrac{1}{8}\rho_G f_{GL}|U_G - U_L|. \qquad [A.3c]$$

The areas per unit volume A_{wL} and A_{GL} are determined by the geometry of the flow regime and channel and are given below.

The friction factors, f_{wL} and f_{GL} are obtained from correlations. The wall-to-liquid friction factor is accurately given by the Blasius (Ueda *et al.* 1977) correlation:

$$f_{wL} = 0.3164\,\mathrm{Re}_L^{-0.25}, \qquad [A.4a]$$

where

$$\mathrm{Re}_L = \frac{\rho_L U_L D_{hywL}}{\mu_L}. \qquad [A.4b]$$

Less is certain about the vapor-to-liquid friction factor which is a function of the geometry of the interface. Correlations available for f_{GL} include those of Wallis (1969), Moeck (1970), Andreussi *et al.* (1985), Cheremisinoff & Davis (1979), Andritsos & Hanratty (1987a,b), Asali *et al.* (1985) and Henstock & Hanratty (1976), and the Eck correlation as reported by Hart *et al.* (1989). The interface friction calculation can account for some information about the interfacial geometry by using criteria about initialization and growth of capillary and roll waves and entrainment of liquid into the gas.

The correlation by Andritsos & Hanratty (1987a) and the Eck correlation (Hart *et al.* 1989) both account for the effects of a rough interface. The former correlation is

$$\frac{f_{GL}}{f_{wG}} = 1 + 15.0\left(\frac{\delta_f}{h}\right)^{1/2}\left(\frac{U_{SG} - U_L}{U_{cl}} - 1\right) \qquad [A.5a]$$

with

$$f_{wG} = 0.184\,\mathrm{Re}_G^{-0.20}, \qquad [A.5b]$$

where $U_{SG} = \alpha_G U_G$ is the critical superficial vapor velocity, and the vapor Reynolds number is

$$\mathrm{Re}_G = \frac{\rho_{Gs} U_G D_{hywG}}{\mu_G}. \qquad [A.5c]$$

The critical superficial velocity for wave growth, U_{cl}, is taken as 5 m/s.

The Eck friction factor correlation (Hart *et al.* 1989) for flow in a rough pipe was modified by Hamersma & Hart (1987) to apply to the interface. Hamersma & Hart related the relative roughness in the correlation to the average film thickness by $k_c = 2.3\,\delta_f$. The Eck correlation for the interface friction factor is

$$f_{GL} = \frac{0.250}{\left[\log_{10}\left(\dfrac{15.0}{\mathrm{Re}_G} + \dfrac{2.3\delta_f}{3.715 D_{hywG}}\right)\right]^2}, \qquad [A.6]$$

where Re_G is as given above.

The geometric parameters for a rectangular flow channel are

$$P_{wL} = (2\delta_f + b), \qquad [A.7a]$$

$$P_{wG} = 2(h - \delta_f) + b, \qquad [A.7b]$$

$$\bar{A}_{wL} = \frac{2\delta_f}{bh} + \frac{1}{h}, \qquad [A.7c]$$

$$\bar{A}_{wG} = \frac{2(h - \delta_f) + b}{bh}, \qquad [A.7d]$$

$$\bar{A}_{GL} = \frac{1}{h}, \tag{A.7e}$$

$$D_{hywL} = \frac{4\alpha_L}{\left(2\frac{\alpha_L}{b} + \frac{1}{h}\right)}, \tag{A.7f}$$

$$D_{hywG} = \frac{4b(h - \delta_f)}{2(h - \delta_f) + b} \tag{A.7g}$$

and

$$D_{hyGL} = 4\alpha_G h. \tag{A.7h}$$

These geometric parameters vary along the channel as the vapor condenses on the liquid.

The equations are solved by a simple first-order finite-difference method. Convergence was determined by changes in the liquid temperature between iterations. With the primary solution variables, other flow parameters are obtained from

$$U_L = \frac{W_L}{(\alpha_L \rho_L A_f)}, \tag{A.8a}$$

$$U_G = \frac{W_G}{(\alpha_G \rho_{Gs} A_f)}, \tag{A.8b}$$

$$\bar{X}_G^w = \frac{W_G}{W} \tag{A.8c}$$

and

$$\alpha_G = \frac{\bar{X}_G^w}{\bar{X}_G^w + \frac{U_G \rho_{Gs}}{U_L \rho_L}(1 - \bar{X}_G^w)}. \tag{A.8d}$$

The thermodynamic state and transport properties are functions of temperature.